

Poly(Styrene Sulfonate)/Poly(Allylamine Hydrochloride) Encapsulation of TiO₂ Nanoparticles Boosts Their Toxic and Repellent Activity Against Zika Virus Mosquito Vectors

Kadarkarai Murugan^{1,2} · Anitha Jaganathan¹ · Rajapandian Rajaganesh¹ · Udaiyan Suresh¹ · Jagan Madhavan² · Sengottayan Senthil-Nathan³ · Aruliah Rajasekar⁴ · Akon Higuchi⁵ · Suresh S. Kumar⁶ · Abdullah A. Alarfaj⁷ · Marcello Nicoletti⁸ · Riccardo Petrelli⁹ · Loredana Cappellacci⁹ · Filippo Maggi⁹ · Giovanni Benelli^{10,11}

Received: 17 July 2017 / Published online: 27 September 2017
© Springer Science+Business Media, LLC 2017

Abstract Green fabricated nanoparticles often need to be encapsulated and stabilized, to ensure uniform dispersion in the aquatic environment and relevant larvicidal activity over time. However, recent research showed that nanoencapsulation processes led to a reduction of nanoparticle larvicidal efficacy. We used an extract of *Argemone mexicana* to reduce TiO₂ nanoparticles, which were then capped with PSS/PAH (poly(styrene sulfonate)/poly(allylamine hydrochloride)). The toxic and repellent potential of the nanoparticles were compared to elucidate their potential effects against the Zika virus vector *Aedes aegypti*. Nanoparticles were characterized by biophysical methods including UV–Vis, EDX and FTIR spectroscopy, SEM, TEM, XRD and DLS analyses. In larvicidal and pupicidal experiments, TiO₂ nanoparticles achieved LC₉₀ values from 41.648 (larva I), to 71.74 ppm (pupa). Nanoencapsulated TiO₂ achieved LC₉₀ values from 39.16

(I), to 69.12 ppm (pupa). In adulticidal experiments, LC₉₀ of TiO₂ nanoparticles on *Ae. aegypti* was 10.31 ppm, while LC₉₀ of nanoencapsulated TiO₂ was 9.54 ppm. At 10 ppm, the repellency towards *Ae. aegypti* was 80.43% for TiO₂ nanoparticles, and 88.04% for nanoencapsulated TiO₂. This research firstly highlighted the promising potential of PSS/PAH encapsulation, leading to the production of highly effective titania nanostructures, if compared to titania nanoparticles synthesized with eco-friendly routes without further stabilization.

Keywords *Aedes aegypti* · *Argemone mexicana* · Dengue fever · Encapsulation · Repellent activity

✉ Kadarkarai Murugan
kmvkvkg@gmail.com

✉ Giovanni Benelli
benelli.giovanni@gmail.com

¹ Division of Entomology, Department of Zoology, School of Life Sciences, Bharathiar University, Coimbatore, Tamil Nadu 641046, India

² Thiruvalluvar University, Serkkadu, Vellore, Tamil Nadu 632115, India

³ Division of Biopesticides and Environmental Toxicology, Sri Paramakalyani Centre for Excellence in Environmental Sciences, Manonmaniam Sundaranar University, Alwarkurichi, Tamil Nadu 627412, India

⁴ Department of Biotechnology, Thiruvalluvar University, Serkkadu, Vellore 632115, India

⁵ Department of Chemical and Materials Engineering, National Central University, No. 300, Jhongli, Taoyuan 32001, Taiwan

⁶ Department of Medical Microbiology and Parasitology, Universiti Putra Malaysia, 43400 Serdang, Selangor, Malaysia

⁷ Department of Botany and Microbiology, College of Science, King Saud University, Riyadh 11451, Saudi Arabia

⁸ Department of Environmental Biology, Sapienza University of Rome, Piazzale Aldo Moro 5, 00185 Rome, Italy

⁹ School of Pharmacy, University of Camerino, Camerino, Italy

¹⁰ Department of Agriculture, Food and Environment, University of Pisa, Via Del Borghetto 80, 56124 Pisa, Italy

¹¹ The BioRobotics Institute, Sant'Anna School of Advanced Studies, Viale Rinaldo Piaggio 34, 56025 Pontedera, Italy

Introduction

Insects are vectors of key diseases leading to significant outbreaks and epidemics in the increasing global populations of humans and animals [10, 58]. Mosquitoes include more than 3500 species. However, less than 100 species, mostly belonging to *Aedes*, *Anopheles* and *Culex* genera, are reported as vectors for diseases that affect humans and other vertebrates. Good examples are malaria, dengue, yellow fever, West Nile, filariasis and Zika virus [16, 78]. These mosquito-borne diseases cause high morbidity and mortality worldwide, and represent a major economic burden within endemic countries [32, 55].

Dengue is primarily transmitted by females of the yellow fever mosquito *Aedes aegypti*, and the Asian tiger mosquito *Aedes albopictus* [18, 76]. *Ae. aegypti* is also a vector for other viral diseases such as yellow fever, chikungunya, and—as showed by recent outbreaks—Zika virus [14]. It is a highly anthropophilic, endophilic, and endophagic day-biting species with an autogenous feeding behavior. This cosmopolitan species can rapidly adapt to different anthropogenic environments. *Ae. aegypti* mosquitoes lay eggs in various aquatic habitats—including small-size ones—such as water-filled plastic containers and tires, tree holes, wells, temporary and permanent pools, and marshy areas, which are often close to human settlements [79].

The first clinically recognized dengue epidemic occurred almost simultaneously in Asia, Africa, and North America in the 1780 s [80]. The World Health Organization estimates that dengue infects approximately 50–400 million people annually in the tropical and subtropical regions [81]. Dengue fever is endemic in Southeast Asian countries including India, Bangladesh, and Pakistan, and its spread is associated with population growth and uncontrolled urbanization in tropical countries, and has become an important public health problem as the number of reported cases continues to increase [14]. Dengue fever is characterized by fever, headache, muscle and joint pains, rash, nausea, and vomiting [58, 59], while more severe forms include dengue hemorrhagic fever and dengue shock syndrome [56].

One of the approaches for the management of mosquito-borne infections is the interruption of disease transmission by killing vectors or preventing mosquitoes from biting [5]. Moreover, due to their low mobility in breeding habitats, young mosquito instars are attractive targets for pest control operations, even if larvicidal treatments are not recommended for rural areas [16]. However, these operations are weakened by the emerging resistance of mosquitoes to synthetic insecticides [35, 49], thus botanical insecticides may be suitable alternative control strategies to pursue

[3, 19, 20, 26, 45, 46, 54, 63, 64, 73]. The massive screening of plant materials and fungi as sources of metabolites for parasitological studies is worthy of attention, as elucidated by the recent example given by Y. Tu, who received the Nobel Prize for her discovery of artemisinin [14]. Notably, plant-borne molecules are often effective at a few parts per million against young instars of *Aedes*, *Anopheles* and *Culex* mosquitoes [11, 52, 53].

Nanotechnology can revolutionize the biomedical, agricultural and veterinary industry [17, 40], leading to the development of novel tools for pest and vector management [9, 15, 50, 57, 72]. Nanoparticles are usually smaller than 100 nm in each spatial dimension, and can be synthesized using top-down and bottom-up strategies. In recent years, the application of nanotechnology in pest management has revolutionized the application of pesticides [6–8, 12, 13, 67, 68]. As arthropod vectors rapidly gain pesticide resistance, there is an urgent need to synthesize novel products via eco-friendly nanosynthesis routes [9, 20].

Titanium dioxide nanoparticles have attracted considerable attention because of their unique physico-optical properties, and are widely used for sunscreen and toothpaste production, surface coating, and water treatment [42]. Constituents from plant extracts can be used to reduce metal ions to nanoparticles in a green single-step synthesis. Recently, researchers proposed the green synthesis of nanomaterials with methods using naturally occurring components such as vitamins, sugars, plant extracts, biodegradable polymers and microorganisms acting as reducing and capping agents [17].

Argemone mexicana L. (Papaveraceae), commonly known as the prickly poppy, is used in folk medicine in several countries [23] for its analgesic, antibacterial, anti-malarial, antispasmodic, sedative and narcotic effects. *A. mexicana* seeds are useful for treating cough and asthma [38] and possess anti-HIV, antioxidant, anxiolytic, hepatoprotective, and sedative activities [4]. Among its main secondary metabolites, benzyloquinoline alkaloids appear to be the most important for the biological activities, namely antimicrobial, antiparasitic, antimalarial, pesticide and neuroprotective ones [60].

Green fabricated nanoparticles often need to be encapsulated and stabilized, to ensure uniform dispersion in the aquatic environment and relevant insecticidal activity over time [21, 22]. Nanoencapsulation is a process through which a chemical such as an insecticide is slowly and efficiently released for insect pest control, allowing proper absorption of the chemical into plants as well as in the aquatic environment [62]. The release mechanisms of nanoencapsulated pesticides include diffusion, dissolution, biodegradation and pH-specific osmosis [25, 75]. Nanoencapsulation has been widely used in biomedicine,

since some of the products are highly tissue-compatible. Besides their potential application as scaffolds in tissue engineering, environmentally sensitive hydrogels, or as sustained-release delivery systems, nanoencapsulated molecules or cells can be used as biosensors, drug carriers and insecticides [44].

However, recent research showed that several nanoencapsulation processes led to a serious reduction of larvicidal efficacy of metal and metal oxide nanoparticles [48]. To face the above mentioned challenge, in this study, we developed a novel titanium dioxide nanocomplex with mosquitocidal potential using *A. mexicana* extracts encapsulated with the polymers poly(styrene sulfonate)/poly(allylamine hydrochloride) (PSS and PAH). Both *A. mexicana*-synthesized TiO₂ nanoparticles and PSS/PAH encapsulated TiO₂ nanoparticles were characterized using UV-visible spectroscopy, Fourier transform infrared spectroscopy (FTIR), X-ray diffraction analysis (XRD), energy-dispersive X-ray analysis (EDX), and field emission scanning electron microscopy (SEM). Furthermore, the toxicity of *A. mexicana*-synthesized TiO₂ nanoparticle and PSS/PAH encapsulated TiO₂ nanoparticles was comparatively assessed on larvae, pupae and adults of the dengue and Zika virus vector *Ae. aegypti*. We also investigated the repellent activity of *A. mexicana*-synthesized TiO₂ nanoparticles and PSS/PAH encapsulated TiO₂ nanoparticles on *Ae. aegypti* adults over different exposure times.

Materials and Methods

Green Synthesis, Encapsulation, and Characterization of TiO₂ Nanoparticles

Fresh *A. mexicana* leaves were collected from the Bharathiar University Campus (Coimbatore, Tamil Nadu, India). The *A. mexicana* leaves were gently washed with tap water and dried in the shade at room temperature, cut into fine pieces, grinded, and sieved to produce a fine powder. Extraction of 50 g of the plant material was performed in 300 mL of methanol for 8 h in a Soxhlet apparatus [77]. The crude plant extract was evaporated to dryness at room temperature.

TiO₂ nanoparticles were synthesized in an Erlenmeyer flask by reacting 0.4 M of titanium tetra-isopropoxide with the *A. mexicana* leaf extract. After 4 h of continuous stirring at 50 °C, the mixture was centrifuged at 5000 rpm for 15 min to obtain a colloidal solution of TiO₂ nanoparticles, which was washed with ethanol and centrifuged at 5000 rpm for 10 min. TiO₂ nanoparticles were separated via annealing at 400 °C in a muffle furnace for 3 h to yield a nanopowder. Experimental concentrations (10, 20, 30,

40, and 50 ppm) were prepared by dilution in distilled water. All stocks and dilutions were stored at -4 °C.

Calcium carbonate (CaCO₃) particles with nano-dispersed diameters were prepared by mixing 0.21 g of Na₂CO₃ and 0.29 g of CaCl₂·5H₂O in 20 mL of H₂O under magnetic agitation with 0.29 g of polystyrene sulfate (PSS). After 30 min, the CaCO₃ particles were centrifuged at 5000 rpm for 10 min and washed in water 3 times. Polyelectrolytes (2 mg/mL) were adsorbed onto the CaCO₃ particles by immersing the particles in 0.1 M of Tris-HCl buffer (pH 7.0) for 15 min followed by three washes in distilled H₂O. The mixture was incubated for 15 min under gentle shaking, and excess electrolytes were removed by centrifugation at 5000 rpm for 10 min and washing in water for 3 h. After assembly of the four subsequent polyelectrolytes bilayers of PSS/PHH/PSS/PAH, the particles were formed by dissolving. The CaCO₃ core was immersed in 0.2 M EDTA solution (100 mL in Tris-HCl buffer at pH 7.0) for 30 min under agitation, and subsequently centrifuged (5000 rpm for 10 min). After washing in water, the hollow microcapsules were re-dispersed in 10 mL of sample solution at a different pH, and the mixture was incubated at room temperature for 15 min. Then, the particles were centrifuged at 5000 rpm for 10 min to remove the suspension.

The presence of *A. mexicana*-synthesized TiO₂ nanoparticles and PSS/PAH encapsulated TiO₂ nanoparticles in the tested preparations was confirmed by sampling the colloidal solutions at regular intervals for UV-Vis analysis using a Shimadzu UV-3600 spectrophotometer scanned from 200 to 700 nm with a resolution of 1 nm. The mixture was then centrifuged at 15,000 rpm for 20 min, the pellet was dissolved in distilled water, then filtered through a 0.45-µm Millipore filter. The morphology of the *A. mexicana*-synthesized TiO₂ nanoparticles and PSS/PAH encapsulated TiO₂ nanoparticles was analyzed using a 10-kV ultra-high-resolution FEI Quanta 200 SEM, where 25 µL of sample were sputter-coated onto a copper stub. The surface groups of the *A. mexicana*-synthesized TiO₂ nanoparticles and PSS/PAH encapsulated TiO₂ nanoparticles were qualitatively confirmed by FTIR spectroscopy [66] using a Perkin-Elmer Spectrum 2000 FTIR spectrophotometer. XRD and EDX were shed light on the crystalline structure and elemental composition of the samples, respectively [67, 68]. TEM was performed using a JEOL 1200 EX microscope operating at an accelerating voltage of 120 kV. Samples were prepared by placing a drop of colloidal solutions of *A. mexicana*-synthesized TiO₂ nanoparticles and PSS/PAH encapsulated TiO₂ nanoparticles on carbon-coated TEM grids. The film on the TEM grid was dried for 5 min under laboratory conditions. The DLS particle size measurements were carried out using a Malvern Zetasizer Nano ZS. Samples were diluted to

0.1 wt% using C12-C15 alkyl benzoate. The measurement duration was set to automatic, and five repeated measurements were taken at 25 °C. The TiO₂ and capped TiO₂ samples were run using the refractive index obtained using Malvern Mastersizer 2000 [2].

Larvicidal, Pupicidal and Adulticidal Activity

Aedes aegypti mosquitoes were reared as reported by Sujitha et al. [70]. Larvicidal and pupicidal assays were conducted in laboratory conditions [27 ± 2 °C, 75–85% R.H., 14:10 (L:D) photoperiod] by testing both *A. mexicana*-synthesized TiO₂ nanoparticles and PSS/PAH encapsulated TiO₂ nanoparticles. Following the method by Murugan et al. [46], in the toxicity tests, 25 first, second, third, fourth and instar larvae and pupae were kept in glass beakers containing 250 mL of dechlorinated water plus the desired concentration of *A. mexicana*-synthesized TiO₂ nanoparticles or PSS/PAH encapsulated TiO₂ nanoparticles. Each dose, as well as the negative control (where no nanoparticles were added) was replicated 5 times. Control mortalities were corrected as indicated by Abbott [1].

In adulticidal assays, based on wide and narrow range tests, *A. mexicana*-synthesized TiO₂ nanoparticles and PSS/PAH encapsulated TiO₂ nanoparticles were tested at 2, 4, 6, 8, and 10 ppm (formulated in 5 ml of aqueous solution), applied on Whatman no. 1 filter papers (size 12 cm × 15 cm). Control papers were treated with distilled water; 20 *Ae. aegypti* females were collected and gently transferred into a plastic holding tube. *Ae. aegypti* females were allowed to acclimatize in the holding tube for 1 h and then exposed to the test paper for 1 h. At the end of the exposure period, the mosquitoes were transferred back to the holding tube for a 24 h recovery period. A cotton pad soaked with 10% of glucose solution was placed on the mesh screen. Each test included a set control groups with five replicates.

Repellent Activity

In repellent assays, a treated and a control cotton pad were soaked with goat blood and placed in opposite directions inside a glass container; then the treated pads were soaked in different concentrations of *A. mexicana* extracts; 20 *Ae. aegypti* females were released into each container, and the number of females landing on each pad was recorded with the slightly modified protocol by Govindarajan and Sivakumar [34]. The repellency of treated and control pads were calculated by the following formula:

$$\frac{C - T}{C} \times 100$$

where C and T is the number of mosquitoes on the control and treated pad, respectively.

Statistical Analysis

Toxicity and repellent data were subjected to ANOVA, then the means were separated by Tukey's HSD test ($P < 0.05$); mosquito mortality data were subjected to probit analysis. LC₅₀ and LC₉₀ were calculated using the method reported by Finney [30]; Chi square values were not significant [15]. Data were analyzed using the SPSS 16.0 software (SPSS Inc., Chicago, IL, USA). A probability level of $P < 0.05$ was used to evaluate the statistical significance of differences between values.

Results

Green Synthesis, Encapsulation, and Characterization of TiO₂ Nanoparticles

The formation and stability of the *A. mexicana*-synthesized TiO₂ nanoparticles was monitored by UV–Vis spectrophotometry, where the UV–Vis spectrum showed a maximum absorbance at 370 nm (Fig. 1a). PSS/PAH encapsulated TiO₂ nanoparticles showed a minimum and maximum absorbance at 148 nm and 370 nm (Fig. 1b), respectively; it was also observed that absorbance increased with the incubation time.

The FTIR spectrum of *A. mexicana*-synthesized TiO₂ nanoparticles indicated several potential functional groups from the *A. mexicana* extracts which probably acted as capping and reducing agents in titania nanosynthesis. Peaks were found at 668 and 1320 cm⁻¹ (Fig. 2a). The stretching frequencies at 1658, 3120, 3468, and 3660 cm⁻¹ can be linked to the presence of organic components in the poppy extract, which were attached to or adsorbed on the surfaces of PSS/PAH encapsulated TiO₂ nanoparticles (Fig. 2b).

The XRD spectrum for *A. mexicana*-synthesized TiO₂ nanoparticles (Fig. 3a) shows five intense peaks with 2θ values of 27°, 41°, 54°, 63°, and 69°, which were assigned to the (101), (100), (111), (211), and (200) planes of the face centered cubic (fcc) phase, which are comparable with the standard (JCPDS 89-3722) TiO₂ lattice. A few unassigned peaks were also seen near these characteristic peaks. For the PSS/PAH encapsulated TiO₂ nanoparticles (Fig. 3b), peaks with 2θ values of 19°, 29°, 26°, 43°, and 54° were assigned to the (100), (101), (111), (201), and (202) planes of the face centered cubic (fcc) phase.

According to SEM and TEM analyses, the morphology of *A. mexicana*-synthesized TiO₂ nanoparticles was mostly rod-shaped; the titania nanoparticles formed aggregates

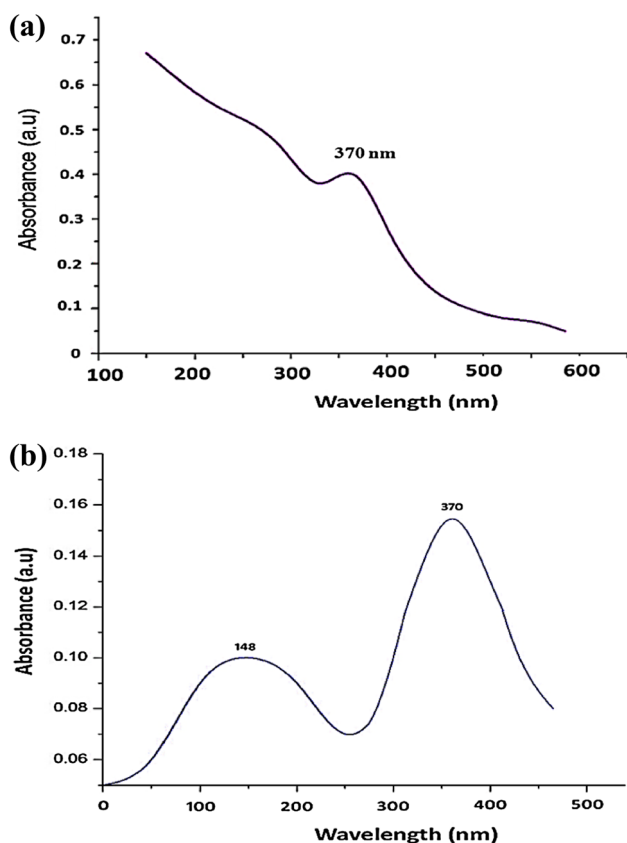


Fig. 1 UV-visible spectra of **a** *Argemone mexicana*-fabricated TiO₂ nanoparticles (120 min after the reaction) and **b** PSS/PAH encapsulated TiO₂ nanoparticles

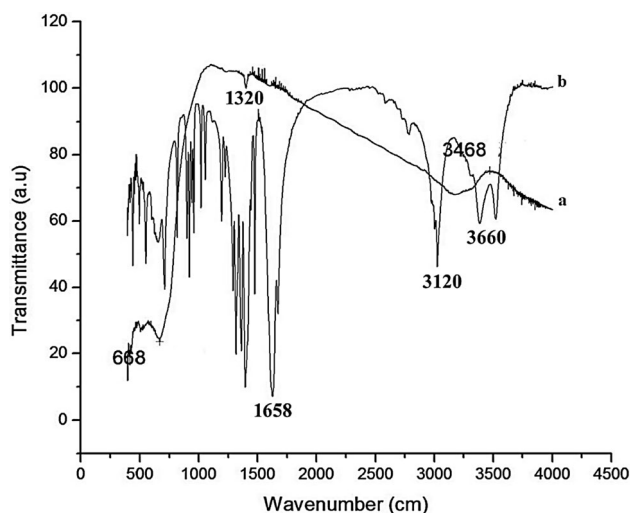


Fig. 2 FT-IR spectra of **a** *Argemone mexicana*-fabricated TiO₂ nanoparticles and **b** PSS/PAH encapsulated TiO₂ nanoparticles

that were about 50 nm in diameter (Figs. 4 and 5). The rod-shaped *A. mexicana*-synthesized TiO₂ nanoparticles (Figs. 4a and 5a) had cubic structures and increased in size to about 65 nm after the encapsulation with PSS/PAH

(Figs. 4b and 5b). Figure 5b shows the morphology of the PSS/PAH encapsulated TiO₂ nanoparticles, formed aggregates of about 40 nm in diameter and TiO₂ exhibited 23 nm.

The TiO₂ nanoparticles generally have a typical absorption peak at 4.9 and 0.1 keV due to the SPR phenomenon. Figure 6 shows a representative EDX profile of the sample spot, showing strong titanium and oxygen signals along with calcium peaks at approximately 0.1, 1, 2, and 4 keV. Overall, strong signals in EDX spectra for Ti and O atoms confirmed the presence of TiO₂ (Fig. 6) in the analyzed samples.

Lastly, from the DLS results given in Fig. 7, it is evident that the particles were dispersed fully and exhibited nano-size lower than 25 nm for *A. mexicana*-synthesized TiO₂ nanoparticles (Fig. 7a) and 45 nm for the PSS/PAH encapsulated TiO₂ nanoparticles (Fig. 7b).

Toxic and Repellent Activity Against *Aedes aegypti*

In larvicidal and pupicidal experiments, *A. mexicana*-synthesized TiO₂ nanoparticles achieved LC₅₀ values of 17.880 (larva I), 21.708 (II), 26.115 (III), 30.045 (IV), and 35.298 ppm (pupa), while the LC₉₀ values were 41.648 (I), 51.148 (II), 56.51 (III), 62.97 (IV), and 71.74 ppm (pupa) (Table 1). Furthermore, PSS/PAH encapsulated TiO₂ nanoparticles achieved LC₅₀ values of 16.154 (I), 21.302 (II), 24.265 (III), 27.550 (IV), and 32.881 ppm (pupa), while the LC₉₀ values were 39.16 (I), 49.94 (II), 53.82 (III), 61.36 (IV), and 69.12 ppm (pupa) (Table 2).

In adulticidal experiments, LC₅₀ and LC₉₀ values of *A. mexicana*-synthesized TiO₂ nanoparticles on *Ae. aegypti* were 3.55 and 10.31 ppm, respectively, while the LC₅₀ and LC₉₀ values of PSS/PAH encapsulated TiO₂ nanoparticles were 3.06 and 9.54 ppm, respectively (Table 3).

In repellence assays, at the maximum concentration tested (10 ppm), the repellency rates calculated on *Ae. aegypti* was significantly lower ($P < 0.05$) for *A. mexicana*-synthesized TiO₂ nanoparticles (80.43%), if compared to that achieved by a single treatment with PSS/PAH encapsulated TiO₂ nanoparticles (88.04%) (Table 4).

Discussion

Green Synthesis, Encapsulation, and Characterization of TiO₂ Nanoparticles

UV-Vis spectroscopy is an essential tool to evaluate the production and stability of metal oxide nanoparticles [31]. The formation of *A. mexicana*-synthesized TiO₂ nanoparticles was confirmed by an absorption peak at 370 nm, while PSS/PAH encapsulated TiO₂ nanoparticles showed a

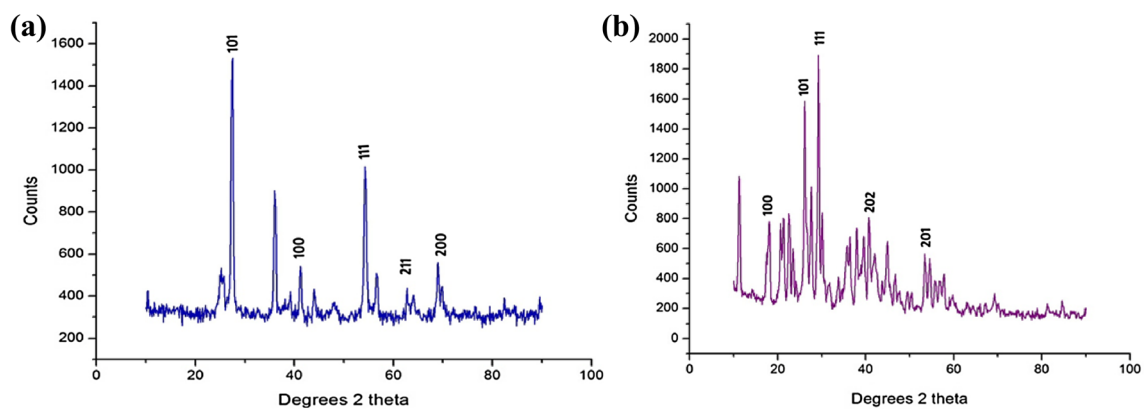


Fig. 3 XRD patterns of **a** *Argemone mexicana*-fabricated TiO₂ nanoparticles and **b** PSS/PAH encapsulated TiO₂ nanoparticles

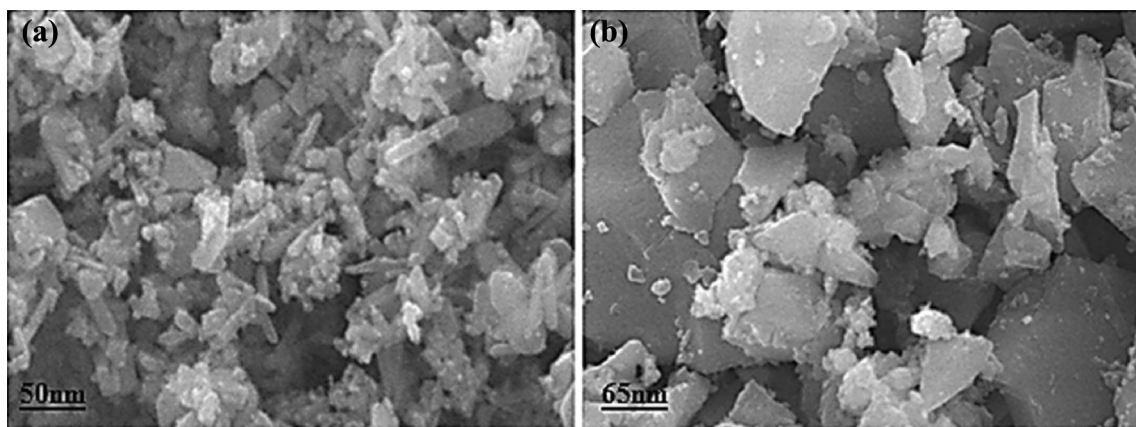


Fig. 4 SEM (20 kV, X30,000) of **a** *Argemone mexicana*-fabricated TiO₂ nanoparticles and **b** PSS/PAH encapsulated TiO₂ nanoparticles

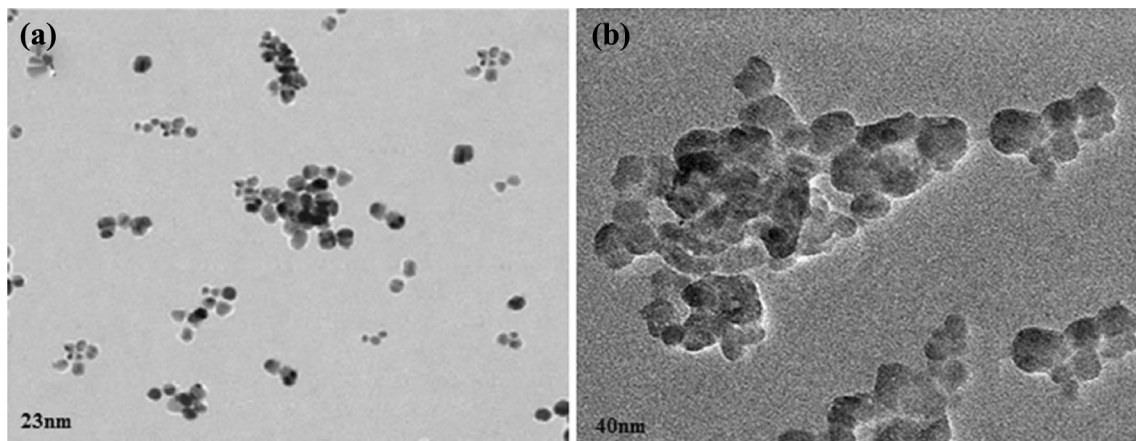


Fig. 5 TEM of **a** *Argemone mexicana*-fabricated TiO₂ nanoparticles and **b** PSS/PAH encapsulated TiO₂ nanoparticles

minimum absorption peak at 148 nm and a maximum absorption peak at 370 nm. Very recently, UV–Vis has been used to study the green synthesis of other metal nanoparticles, including silver and gold ones. About the latter, a recent example has been provided by Murugan et al. [46], which studied the UV–Vis spectrum of gold

nanoparticles synthesized using *Cymbopogon citratus* (DC.) Stapf, where the formation of Au nanostructures was confirmed by the presence of an absorption peak at 540 nm.

Concerning the functional groups from the *A. mexicana* extract, which were probably involved in the reduction of

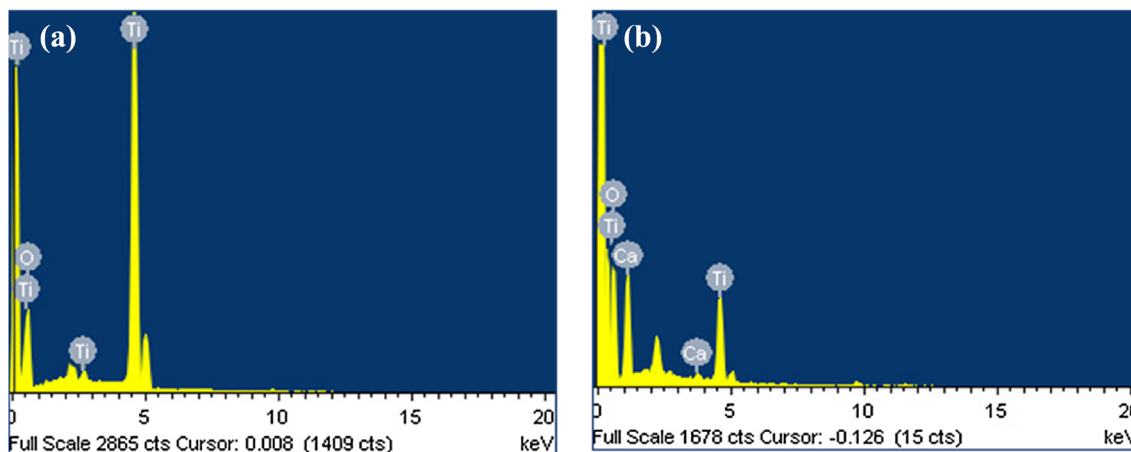


Fig. 6 EDX profiles of **a** *Argemone mexicana*-fabricated TiO₂ nanoparticles and **b** PSS/PAH encapsulated TiO₂ nanoparticles

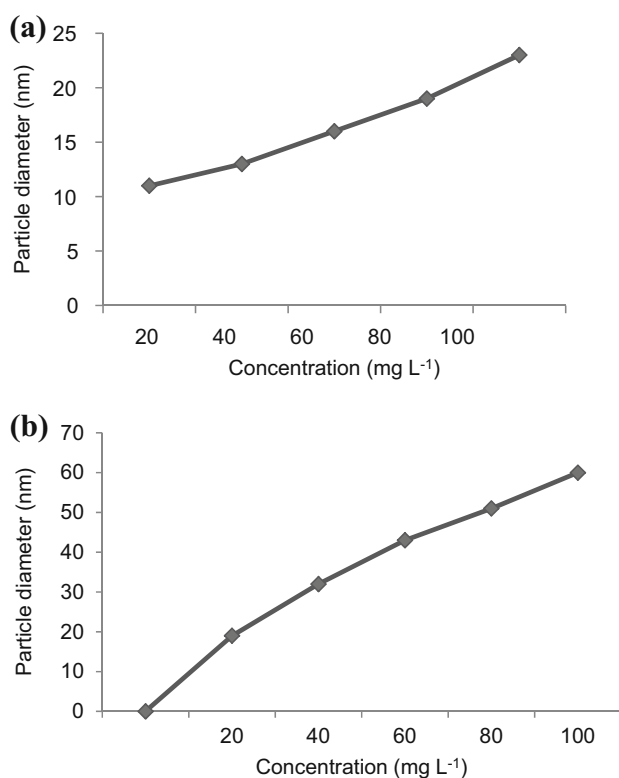


Fig. 7 Dynamic light scattering (DLS) showing particle size of **a** *Argemone mexicana*-fabricated TiO₂ nanoparticles and **b** PSS/PAH encapsulated TiO₂ nanoparticles

TiO₂ nanoparticles, the FTIR peak at 668 cm⁻¹ may be linked with the formation of C–Br bonds, while the peak at 1320 cm⁻¹ may indicate C=O bonds. The peak sat 1658, 3120, 3468, and 3660 cm⁻¹ were probably due to the formation of C=C, C–H, O–H, and O–H bonds, respectively [41, 69]. Based on this information, it was argued that various concentrations of alcohols, phenols, and alkenes were still present in the colloidal solution after the formation of PSS/PAH encapsulated TiO₂ nanoparticles.

Furthermore, the XRD pattern of *A. mexicana*-synthesized TiO₂ nanoparticles showed 5 intense peaks at 27°, 41°, 54°, 63°, and 69°, while the XRD pattern of PSS/PAH encapsulated TiO₂ nanoparticles had peaks at 19°, 29°, 26°, 43°, and 54°. Recently, several XRD studies have been carried out to shed light on the crystalline structure of mosquitocidal nanoparticles [13, 71, 74], including titania nanostructures [47]. Concerning other metal nanoparticles, several studies are available. For example, Madhiyazhagan et al. [41], studied the XRD pattern of Ag nanoparticles synthesized using the extract of the seaweed *Sargassum muticum*; results showed five high diffraction peaks at 45.6°, 51.3°, 58.1°, 66.5°, and 71.1°, indexing the Bragg reflection planes (004), (112), (103), (104), and (006), respectively.

SEM studies pointed out that the reduced *A. mexicana*-synthesized TiO₂ nanoparticles were observed to be mostly rod-shaped, with aggregates always lower of 50 nm in size; on the other hand, encapsulated PSS/PAH encapsulated TiO₂nanoparticles were cubic, with a size of about 65 nm. In both samples, EDX assays revealed the presence of strong Ti and O peaks. The increase in particle diameter confirmed the encapsulation of TiO₂ nanoparticles by PSS/PAH. Notably, the present green synthesis protocol led to the production of titania nanoparticles with different features if compared with the ones synthesized via classic methods, such has hydrothermal synthesis. Indeed, at variance with our results, Murugan et al. [47] showed that titania nanoparticles fabricated via hydrothermal synthesis and analyzed by FESEM showed spherical shapes, not rod-like ones, with a wider size range (i.e. from 20 to 100 nm). These data represent a further evidence of the great potential of plant-mediated green synthesis routes, that can be easily carried out to produce nanoparticles with different features if compared with those obtained with chemical and physical methods (see [21, 22] for recent reviews).

Table 1 Larvicidal and pupicidal toxicity of *Argemone mexicana*-synthesized TiO₂ nanoparticles against the dengue and Zika virus vector *Aedes aegypti*

| Target | LC ₅₀ (LC ₉₀) (ppm) | 95% Confidence limit LC ₅₀ (LC ₉₀) | | Regression equation | χ^2 (d.f. = 4) |
|-----------|--|---|-----------------|-----------------------|-----------------------|
| | | 95% LCL | 95% UCL | | |
| Larva I | 17.880 (41.648) | 14.769 (38.232) | 20.428 (46.294) | $y = -0.964 + 0.054x$ | 3.042 ^{n.s.} |
| Larva II | 21.708 (51.148) | 18.337 (46.425) | 24.538 (57.946) | $y = -0.945 + 0.044x$ | 0.598 ^{n.s.} |
| Larva III | 26.115 (56.514) | 23.071 (51.156) | 28.900 (64.327) | $y = -1.101 + 0.042x$ | 0.359 ^{n.s.} |
| Larva IV | 30.045 (62.971) | 26.996 (56.448) | 33.100 (72.825) | $y = -1.169 + 0.039x$ | 0.325 ^{n.s.} |
| Pupa | 35.298 (71.742) | 32.004 (63.292) | 39.133 (85.195) | $y = -1.241 + 0.035x$ | 0.834 ^{n.s.} |

^{n.s.}Not significant ($P > 0.05$)

Table 2 Larvicidal and pupicidal toxicity of PSS/PAH encapsulated *Argemone mexicana*-synthesized TiO₂ nanoparticles against the dengue and Zika virus vector *Aedes aegypti*

| Target | LC ₅₀ (LC ₉₀) (ppm) | 95% Confidence limit LC ₅₀ (LC ₉₀) | | Regression equation | χ^2 (d.f. = 4) |
|-----------|--|---|-----------------|-----------------------|-----------------------|
| | | 95% LCL | 95% UCL | | |
| Larva I | 16.154 (39.165) | 12.907 (35.920) | 18.750 (43.568) | $y = -0.900 + 0.056x$ | 5.203 ^{n.s.} |
| Larva II | 21.302 (49.946) | 17.980 (45.420) | 24.083 (56.410) | $y = -0.953 + 0.045x$ | 1.486 ^{n.s.} |
| Larva III | 24.265 (53.823) | 21.155 (48.844) | 27.011 (61.009) | $y = -1.052 + 0.043x$ | 0.705 ^{n.s.} |
| Larva IV | 27.550 (61.361) | 24.282 (54.887) | 30.615 (71.223) | $y = -1.044 + 0.038x$ | 0.381 ^{n.s.} |
| Pupa | 32.881 (69.120) | 29.622 (61.129) | 36.433 (81.750) | $y = -1.163 + 0.035x$ | 1.120 ^{n.s.} |

^{n.s.}Not significant ($P > 0.05$)

Concerning other metal nano-complexes obtained with green synthesis routes, Suresh et al. [71] reported that SEM of green synthesized Ag⁰ nanoparticles showed spherical shapes with an average size of 30–60 nm.

Various attempts have been conducted also to microencapsulate plant-borne products. For instance, Hsieh et al. [37] applied thermal treatments to study the controlled release properties of chitosan-microencapsulated citronella oil, while Mourtzinos et al. [43] encapsulated olive leaf extracts in β -cyclodextrin substrates. In the present investigation, the adoption of DLS showed the nano-particle size of both green synthesized and capped nanoparticle. DLS is an efficient and convenient method to analyze the particle size of nanoparticles [48]. Hence, here DLS has been applied to support TEM data on the size of synthesized nanotitania. Notably, suspensions tested in DLS measurements are often treated with a standard dispersant to give good or at least reproducible dispersions [28]. If this is not carried out, and the sample is simply dispersed in deionized water, the measured size may vary significantly with the tested particle concentration, and because the particle concentration is often adjusted to give optimum obscuration, significant variability of the results may occur. A similar dependence has been reported for

5 nm TiO₂ particles by Fatissou et al. [29]. Moreover, Patri et al. [51] have reported large differences for bigger TiO₂ particles, i.e., about 120 nm at low ionic strength (10 mM NaCl) and 1000–2000 nm in solutions showing high ionic strength.

Toxic and Repellent Activity Against *Aedes aegypti*

The experiments conducted on larval and pupal stages of the dengue and Zika virus vector *Ae. aegypti* showed a relevant toxicity of both *A. mexicana*-synthesized TiO₂ nanoparticles and PSS/PAH encapsulated TiO₂ nanoparticles. Notably, the LC₅₀ values of *A. mexicana*-synthesized TiO₂ nanoparticles (i.e., from 17.880 ppm on first instar larvae to 35.298 ppm on pupae) were slightly higher if compared with PSS/PAH encapsulated TiO₂ nanoparticles (i.e., from 16.154 ppm on first instar larvae to 32.881 ppm on pupae). Moreover, the same trend was confirmed in adulticidal experiments, where *A. mexicana*-synthesized TiO₂ nanoparticles had a LC₅₀ of 3.55 ppm, while PSS/PAH encapsulated TiO₂ nanoparticles had slightly lower LC₅₀ (3.06 ppm). Notably, also in repellence assays, the repellency rates calculated on *Ae. aegypti* were lower for *A. mexicana*-synthesized TiO₂ nanoparticles (80.43%) if

Table 3 Adulticidal activity of *Argemone mexicana*-synthesized titanium nanoparticles and PSS/PAH encapsulated TiO₂ nanoparticles against the dengue and Zika virus vector *Aedes aegypti*

| Treatment | Mortality (%) (mean ± SD) | | | | | LC ₅₀ (95% LCL–UCL) | LC ₉₀ (95% LCL–UCL) | χ^2 (d.f = 4) |
|---|---------------------------|-------------|-------------|-------------|-------------|--------------------------------|--------------------------------|-----------------------|
| | Control | 2 ppm | 4 ppm | 6 ppm | 8 ppm | | | |
| TiO ₂ nanoparticles | 0.0 | 40.6 ± 2.41 | 53.2 ± 1.92 | 64.6 ± 2.07 | 78.8 ± 1.92 | 91.2 ± 2.59 | 10.31 (9.23–11.96) | 1.310 ^{n.s.} |
| PSS/PAH encapsulated TiO ₂ nanoparticles | 0.0 | 44.2 ± 2.39 | 56.4 ± 2.70 | 68.8 ± 2.59 | 82.6 ± 2.07 | 93.6 ± 2.41 | 9.546 (8.574–11.000) | 1.420 ^{n.s.} |

^{n.s.}Not significant ($P > 0.05$)

compared to PSS/PAH encapsulated TiO₂ nanoparticles (88.04%).

To our mind, these findings represent a rather rare evidence in the field of green nanosynthesis of mosquito-cidal nanoparticles. Indeed, earlier attempts failed to maintain the high insecticidal activity of green synthesized nanoparticles after the encapsulation process; very recently, Murugan et al. [48] proposed the bio-encapsulation of chitosan-Ag nanocomplex, showing activity against *Anopheles stephensi* malaria vectors in laboratory and in the field. Both nano-products also reduced longevity and fecundity of *An. stephensi*. The bioencapsulated chitosan-Ag nanocomplex showed a lower larvicidal and pupicidal toxicity (LC₅₀ range: 54.65–98.17 ppm) if compared with non-encapsulated chitosan-fabricated Ag nanoparticles (LC₅₀ range: 4.43–7.64 ppm) [48]. When comparing the toxicities of non-encapsulated and encapsulated *A. mexicana*-TiO₂ nanoparticles, the increase of toxicity detected here was in accordance with the findings by Cheung and Hammockm [24], who carried out the micro-lipid droplet encapsulation of *Bacillus thuringiensis* subsp. *israelensis* endotoxins, reporting its toxicity against the larvae of four mosquito species, i.e., *Ae. aegypti*, *An. freeborni*, *Cx. pipiens* and *Cx. tarsalis*. Later, Hadapad et al. [36] evaluated the residual activity of sustained-release biopolymer-based formulations for *B. sphaericus* strains against *Cx. quinquefasciatus* larvae. The present work reports an eco-friendly and simple method allowing the encapsulation of titania nanoparticles without lowering their mosquito-cidal activity against the dengue and Zika virus vector *Ae. aegypti*.

More generally, in the latest years, a wide number of green routes aimed at the production of nanoparticles toxicity to various mosquito species have been developed. Most of the studies focused on the toxicity of plant-synthesized metal nanoparticles, with special reference to silver ones [12, 39, 65]. On the other hand, only few researches focused on the toxicity of titania nanoparticles against mosquito young instars [47]. Besides plant-based fabrication processes, bacterial and fungal extract have also been employed to prepare various metal nanoparticles. For example, Ag nanoparticles have been fabricated using extracts of the filamentous fungus *Cochliobolus lunatus* and then tested against *Ae. aegypti* II–IV larval instars, achieving LC₅₀ of 1.29, 1.48, and 1.58 ppm, respectively [61].

In addition to being used as reducing and capping agents for nanosynthesis, a number of phytochemicals have been tested for their mosquito larvicidal, adulticidal and repellent properties [27, 33]. The review by Pavea [52] recently highlighted that several plant-borne compounds showed relevant activity as mosquito larvicides. Also, Amerasan et al. [3] studied the adulticidal activity of

Table 4 Repellent activity (%) of *Argemone mexicana*-synthesized titanium nanoparticles (NP) and PSS/PAH encapsulated titanium nanoparticles (eNP) against the dengue and Zika virus vector *Aedes aegypti*

| Activity (h) | Control | | 2 ppm | | 4 ppm | | 6 ppm | | 8 ppm | | 10 ppm | |
|------------------|-----------|--------------------|-------------------|--------------------|--------------------|--------------------|--------------------|--------------------|--------------------|--------------------|--------------------|-----|
| | NP | eNP | NP | eNP | NP | eNP | NP | eNP | NP | eNP | NP | eNP |
| 10.00–11.00 | 30 ± 3.60 | 27 ± 2.64 | 26 ± 1.73 | 22 ± 2.64 | 20 ± 2.00 | 17 ± 5.29 | 14 ± 4.35 | 12 ± 1.00 | 10 ± 2.82 | 8 ± 4.00 | 5 ± 0.70 | |
| 12.00–13.00 | 25 ± 0.57 | 22 ± 1.73 | 21 ± 2.00 | 19 ± 5.29 | 16 ± 4.58 | 15 ± 4.00 | 11 ± 1.73 | 10 ± 2.64 | 7 ± 0.00 | 5 ± 1.00 | 4 ± 1.41 | |
| 14.00–15.00 | 18 ± 3.60 | 15 ± 4.58 | 14 ± 1.41 | 12 ± 2.00 | 10 ± 2.82 | 10 ± 1.00 | 6 ± 1.41 | 8 ± 2.64 | 3 ± 1.41 | 3 ± 1.00 | 2 ± 1.41 | |
| 16.00–17.00 | 12 ± 0.00 | 10 ± 1.00 | 7 ± 3.00 | 8 ± 1.73 | 4 ± 0.00 | 5 ± 2.64 | 2 ± 0.70 | 3 ± 1.73 | 1 ± 0.70 | 2 ± 0.00 | 0 ± 0.00 | |
| 18.00–19.00 | 7 ± 2.00 | 6 ± 0.00 | 5 ± 2.64 | 4 ± 0.00 | 4 ± 2.64 | 2 ± 1.00 | 2 ± 0.00 | 1 ± 0.57 | 0 ± 0.00 | 0 ± 0.00 | 0 ± 0.00 | |
| Fed mosquitoes | 92 ± 2.00 | 79 ± 1.00 | 73 ± 1.00 | 65 ± 4.00 | 54 ± 3.46 | 49 ± 1.00 | 35 ± 0.70 | 34 ± 3.60 | 21 ± 2.82 | 18 ± 2.00 | 11 ± 2.82 | |
| Unfed mosquitoes | 8 ± 2.64 | 21 ± 1.00 | 24 ± 4.58 | 35 ± 1.00 | 46 ± 2.0 | 51 ± 3.60 | 65 ± 2.82 | 66 ± 3.60 | 79 ± 1.41 | 82 ± 2.00 | 89 ± 2.82 | |
| Protection (%) | – | 14.13 ^a | 20.6 ^b | 29.35 ^c | 41.30 ^d | 46.74 ^e | 61.96 ^f | 63.04 ^f | 77.17 ^g | 80.43 ^g | 88.04 ^h | |

Within the row, means followed by the same letter(s) are not significantly different (ANOVA, Tukey's HSD test, $P < 0.05$)

Senna tora (L.) Roxb. extracts in hexane, chloroform, benzene, acetone, and methanol against *Ae. aegypti*. The adulticidal activity of the essential oil of *Lantana camara* L. was evaluated against five mosquito species, *Ae. aegypti*, *Cx. quinquefasciatus*, *An. culicifacies*, *Ancylos fluvialitis*, and *An. stephensi*, on impregnated papers at concentrations of 0.208 mg/cm², where the KDT₅₀ and KDT₉₀ values of the oil were 20, 18, 15, 12, and 14 min and 35, 28, 25, 18, and 23 min, respectively; mortality percentages for each species were 93.3, 95.2, 100, 100, and 100%, respectively [26]. However, on the other hand, our knowledge about the adulticidal potential of green synthesized nanoparticles remains scarce, if compared with research efforts on their larvicidal and pupicidal potential [12, 39].

Conclusions

Overall, here we used the poppy species *A. mexicana* to reduce titanium dioxide nanoparticles, which were then capped with PSS/PAH. The toxicity and repellent potential of both nanoparticles were compared to elucidate their potential effects against the dengue and Zika virus vector *Ae. aegypti*. At variance with earlier studies, this research firstly highlighted the highly promising potential of PSS/PAH encapsulation. This process led to the production of highly stable encapsulated titania nanostructures showing higher toxicity and repellent potential against *Ae. aegypti*, if compared with titania nanoparticles synthesized with eco-friendly routes without further stabilization.

Acknowledgements The authors extend their appreciation to the International Scientific Partnership Program ISPP at King Saud University for funding this research work through ISPP# 0062. Dr. Anitha Jaganathan is grateful to the University Grant Commission (New Delhi, India), Project No. PDFSS-2014-15-SC-TAM-10125.

Compliance with Ethical Standards

Conflict of interest The authors declare that they have no conflict of interest.

References

1. W. S. Abbott (1925). A method of computing the effectiveness of insecticides. *J. Econ. Entomol.* **18**:267–269.
2. Z. Abbas, J. P. Holmberg, A. K. Hellstrom, M. Hagstrom, J. Bergenhol, M. Hasselov and Ahlberg (2011). Synthesis, characterization and particle size distribution of TiO₂ colloidal nanoparticles. *Colloids Surf. A.* **384**, 254–261.
3. D. Amerasan, K. Murugan, K. Kovendan and P. Mahesh Kumar (2012). Adulticidal and repellent properties of *Cassia tora* Linn. (Family: Caesalpinaceae) against *Culex quinquefasciatus*, *Aedes aegypti*, and *Anopheles stephensi*. *Parasitol. Res.* **111**, 1953–1964.
4. A. S. Apu, S. H. Bhuyan and M. Matin (2012). Phytochemical analysis and bioactivities of *Argemone mexicana* Linn. leaves. *Pharmacol.OnLine.* **3**, 16–23.
5. S. Arokiyaraj, V. D. Kumar, V. Elakya, T. S. Kamala, S. K. Park, M. Ragam, M. Saravanan, M. Bououdina, M. V. Arasu, K. Kovendan and S. Vincent (2011). Biosynthesized silver nanoparticles using floral extract of *Chrysanthemum indicum* L.—potential for malaria vector control. *Environ. Sci. Pollut. Res.* doi:10.1007/s11356-015-4148-9.
6. R. M. S. T. Azarudeen, M. Govindarajan, A. Amsath, S. Kadaikunnan, N. S. Alharbi, P. Vijayan, U. Muthukumaran and G. Benelli (2016). Size-controlled fabrication of silver nanoparticles using the *Hedyotis puberula* leaf extract: toxicity on mosquito vectors and impact on biological control agents. *RSC Adv.* **6**, 96573–96583.
7. R. M. S. T. Azarudeen, M. Govindarajan, A. Amsath, U. Muthukumaran and G. Benelli (2017a). Single-step biofabrication of silver nanocrystals using *Naregamia alata*: a cost effective and eco-friendly control tool in the fight against malaria, Zika virus and St. Louis encephalitis mosquito vectors. *J. Clust. Sci.* **28**, 179–203.
8. R. M. S. T. Azarudeen, M. Govindarajan, M. M. AlShebly, F. S. AlQahtani, A. Amsath and G. Benelli (2017b). One pot green synthesis of colloidal silver nanocrystals using the *Ventilago maderaspatana* leaf extract: acute toxicity on malaria, Zika virus and filariasis mosquito vectors. *J. Clust. Sci.* **28**, 369–392.
9. B. Banumathi, B. Vaseeharan, R. Periyannan, N. M. Prabhu, P. Ramasamy, K. Murugan, A. Canale and G. Benelli (2017). Exploitation of chemical, herbal and nanoformulated acaricides to control the cattle tick, *Rhipicephalus (Boophilus) microplus*—a review. *Vet. Parasitol.* **244**, 102–110.
10. G. Benelli (2015a). Research in mosquito control: current challenges for a brighter future. *Parasitol. Res.* **114**, 2801–2805.
11. G. Benelli (2015b). Plant-borne ovicides in the fight against mosquito vectors of medical and veterinary importance: a systematic review. *Parasitol. Res.* **114**, 3201–3212.
12. G. Benelli (2016a). Plant-mediated biosynthesis of nanoparticles as an emerging tool against mosquitoes of medical and veterinary importance: a review. *Parasitol. Res.* **115**, 23–34.
13. G. Benelli (2016b). Green synthesized nanoparticles in the fight against mosquito-borne diseases and cancer—a brief review. *Enzyme Microb. Technol.* **95**, 58–68.
14. G. Benelli and H. Mehlhorn (2016). Declining malaria, rising of dengue and Zika virus: insights for mosquito vector control. *Parasitol. Res.* **115**, 1747–1754.
15. G. Benelli (2017). Commentary: data analysis in bionanoscience issues to watch for. *J. Clust. Sci.* doi:10.1007/s10876-016-1143-3.
16. G. Benelli and J. Beier (2017). Current vector control challenges in the fight against malaria. *Acta Trop.* **174**, 91–96.
17. G. Benelli and C. M. Lukehart (2017). Special issue: applications of green-synthesized nanoparticles in pharmacology, parasitology and entomology. *J. Clust. Sci.* **28**, 1–2.
18. G. Benelli and D. Romano (2017). Mosquito vectors of Zika virus. *Entomol. Gen.* doi: 10.1127/entomologia/2017/0496.
19. G. Benelli, A. Canale, C. Toniolo, A. Higuchi, K. Murugan, R. Pavela and M. Nicoletti (2017a). Neem (*Azadirachta indica*): towards the ideal insecticide?. *Nat. Prod. Res.* **31**, 369–386.
20. G. Benelli, F. Maggi, D. Romano, C. Stefanini, B. Vaseeharan, S. Kumar, A. Higuchi, A. A. Alarfaj, H. Mehlhorn and A. Canale (2017b). Nanoparticles as effective acaricides against ticks—a review. *Ticks Tick-borne Dis.* doi:10.1016/j.ttbdis.2017.08.004.
21. G. Benelli, R. Pavela, F. Maggi, R. Petrelli and M. Nicoletti (2017c). Commentary: making green pesticides greener? The potential of plant products for nanosynthesis and pest control. *J. Clust. Sci.* **28**, 3–10.

22. G. Benelli, F. Maggi, R. Pavela, K. Murugan, M. Govindarajan, B. Vaseeharan, R. Petrelli, L. Cappellacci, S. Kumar, A. Hofer, M. R. Youssefi, A. A. Alarfaj, J. S. Hwang and A. Higuchi (2017d). Mosquito control with green nanopesticides: towards the one health approach? A review of non-target effects. *Environ. Sci. Pollut. Res.* doi:10.1007/s11356-017-9752-4.
23. I. Bhattacharjee, S. K. Chatterjee and G. Chandra (2010). Isolation and identification of antibacterial components in seed extracts of *Argemone mexicana* L. (Papaveraceae). *Asian Pac. J. Trop. Med.* **3**, 547–551.
24. P. Y. K. Cheung and B. D. Hammock (1985). Micro-lipid droplet encapsulation of *Bacillus thuringiensis* subsp. *israelensis* b-endotoxin for control of mosquito larvae. *Appl. Environ. Microbiol.* **50**, 984–988.
25. W. K. Ding and N. P. Shah (2009) Effect of various encapsulating materials on the stability of probiotic bacteria. *J. Food Sci.* **74**, 100–107.
26. V. K. Dua, A. C. Pandey and A. P. Dash (2010). Adulticidal activity of essential oil of *Lantana camara* leaves against mosquitoes. *Indian J. Med. Res.* **131**, 434–439.
27. E. S. Edwin, P. Vasantha-Srinivasan, S. Senthil-Nathan, A. Thanigaivel et al. (2016). Anti-dengue efficacy of bioactive andrographolide from *Andrographis paniculata* (Lamiaceae) against the primary dengue vector *Aedes aegypti* (Diptera: Culicidae). *Acta Trop.* **163**, 167–178.
28. T. A. Egerton and I. R. Tooley (2011). Physical characterization of titanium dioxide nanoparticles. *Int. J. Cosmet. Sci.* doi:10.1111/ics.12113.
29. J. Fatisson, R. F. Domingos, K. J. Wilkinson and N. Tufenkji (2009). Deposition of TiO₂ nanoparticles onto silica measured using a quartz crystal microbalance with dissipation monitoring. *Langmuir* **25**, 6062–6069.
30. D. J. Finney, *Probit Analysis* (Cambridge University, London, 1971), pp. 68–78.
31. D. S. Goodsell, *Bionanotechnology: Lessons From Nature* (Wiley, Hoboken, 2004).
32. C. A. Guerra, R. W. Snow and S. I. Hay (2006). A global assessment of closed forests, deforestation and malaria risk. *Ann. Trop. Med. Parasitol.* **100**, 189–204.
33. M. Govindarajan (2010). Larvicidal and repellent activities of *Sida acuta* Burm. F. (Family: Malvaceae) against three important vector mosquitoes. *Asian Pac. J. Trop. Biomed.* **3**, 691–695.
34. M. Govindarajan and R. Sivakumar (2011). Mosquito adulticidal and repellent activities of botanical extracts against malarial vector, *Anopheles stephensi* Liston (Diptera: Culicidae). *Asian Pac. J. Trop. Med.* **2011**, 941–947.
35. J. Hemingway and H. Ranson (2000). Insecticide resistance in insect vectors of human disease. *Annu. Rev. Entomol.* **45**, 371–391.
36. A. B. Hadapad, R. S. Hire, N. Vijayalakshmi and T. K. Dongre (2011). Sustained-release biopolymer based formulations for *Bacillus sphaericus* Neide ISPC-8. *J. Pest Sci.* doi:10.1007/s10340-010-0347-9.
37. W. C. Hsieh, C. P. Chang and Y. L. Gao (2006). Controlled release properties of chitosan encapsulated volatile *Citronella* oil microcapsules by thermal treatments. *Colloid Surf. B Biointerfaces* **53**, 209–214.
38. G. Ji, P. Dwivedi, S. Sundaram and R. Prakash (2015). Aqueous extract of *Argemone mexicana* roots for effective protection of mild steel in an HCl environment. *Res. Chem. Intermed.* **42**, 439–459.
39. K. Kovendan, K. Murugan, P. Mahesh Kumar, P. Thiyagarajan and S. J. William (2012). Ovicidal, repellent, adulticidal and field evaluations of plant extract against dengue, malaria and filarial vectors. *Parasitol. Res.* **112**, 1205–1219.
40. R. Kumar, M. Sharon and A. K. Choudhary (2010). Nanotechnology in agricultural diseases and food safety. *J. Phytol.* **2**, 83–92.
41. P. Madhiyazhagan, K. Murugan, A. Naresh Kumar, T. Nataraj, D. Dinesh, C. Panneerselvam, J. Subramaniam, P. Mahesh Kumar, U. Suresh, M. Roni, M. Nicoletti, A. A. Alarfaj, A. Higuchi, M. A. Munusamy and G. Benelli (2015). *Sargassum muticum*-synthesized silver nanoparticles: an effective control tool against mosquito vectors and bacterial pathogens. *Parasitol. Res.* doi:10.1007/s00436-015-4671-0.
42. W. Miao, B. Zhu, X. Xiao, Y. Li, N. B. Dirbaba, B. Zhou and H. Wu (2015). Effects of titanium dioxide nanoparticles on lead bioconcentration and toxicity on thyroid endocrine system and neuronal development in zebrafish larvae. *Aquat. Toxicol.* **161**, 117–126.
43. I. Mourtzinou, F. Salta, K. Yannakopoulou, A. Chiou and V. T. Karathanos (2007). Encapsulation of olive leaf extract in betacyclodextrin. *J. Agric. Food. Chem.* **55**, 8088–8894.
44. W. E. G. Muller, S. Engel, X. Wang, S. E. Wolf and W. Tremel (2008). Bioencapsulation of living bacteria (*Escherichia coli*) with poly (silicate) after transformation with silicate in-a gene. *Biomaterials.* **29**, 771–779.
45. K. Murugan, G. Benelli, A. Suganya, D. Dinesh, C. Panneerselvam, M. Nicoletti, J. S. Hwang, P. Mahesh Kumar, J. Subramaniam and U. Suresh (2015a). Toxicity of seaweed-synthesized silver nanoparticles against the filariasis vector *Culex quinquefasciatus* and its impact on predation efficiency of the cyclopoid crustacean *Mesocyclops longisetus*. *Parasitol. Res.* **114**, 2243–2253.
46. K. Murugan, G. Benelli, C. Panneerselvam, J. Subramaniam, T. Jeyalalitha, D. Dinesh, M. Nicoletti, J. S. Hwang, U. Suresh and P. Madhiyazhagan (2015b). *Cymbopogon citratus*-synthesized gold nanoparticles boost the predation efficiency of copepod *Mesocyclops aspericornis* against malaria and dengue mosquitoes. *Exp. Parasitol.* **153**, 129–138.
47. K. Murugan, D. Dinesh, K. Kavithaa, M. Paulpandi, T. Ponraj, M. S. Alsalthi, S. Devanesan, J. Subramaniam, R. Rajaganesh, H. Wei, K. Suresh, M. Nicoletti and G. Benelli (2016). Hydrothermal synthesis of titanium dioxide nanoparticles: mosquitocidal potential and anticancer activity on human breast cancer cells (MCF-7). *Parasitol. Res.* **115**, 1085–1096.
48. K. Murugan, A. Jaganathan, U. Suresh, R. Rajaganesh, S. Jayasanthini, A. Higuchi, S. Kumar and G. Benelli (2017). Towards bio-encapsulation of chitosan-silver nanocomplex? Impact on malaria mosquito vectors, human breast adenocarcinoma cells (MCF-7) and behavioral traits of non-target fishes. *J. Clust. Sci.* **28**, 529–550.
49. M. N. Naqqash, A. Gokce, A. Bakhsh and M. Salim (2016). Insecticide resistance and its molecular basis in urban insect pests. *Parasitol. Res.* **115**, 1363–1373.
50. J. D. Patel, U. Panchal, M. Panchal and B. A. Makwana (2015). Green synthesis of silver nanoparticles using the leaf extract and their microbial activity. *J. Adv. Chem. Sci.* **1**, 82–85.
51. A. Patri, T. Umbreit, J. Zheng, K. Nagashima, P. Goering, S. Francke-Carroll, E. Gordon, J. Weaver, T. Miller, N. Sadrieh, S. McNeil and M. Stratmeyer (2009). Energy dispersive X-ray analysis of titanium dioxide nanoparticle distribution after intravenous and subcutaneous injection in mice. *J. Appl. Toxicol.* **29**, 662–672.
52. R. Pavela (2015a). Essential oils for the development of eco-friendly mosquito larvicides: a review. *Ind. Crops Prod.* **76**, 174–187.
53. R. Pavela (2015b). Acute toxicity and synergistic and antagonistic effects of the aromatic compounds of some essential oils against *Culex quinquefasciatus* Say larvae. *Parasitol. Res.* doi:10.1007/s00436-015-4614-9.

54. R. Pavela and G. Benelli (2016a). Ethnobotanical knowledge on botanical repellents employed in the African region against mosquito vectors – a review. *Exp. Parasitol.* **167**:103–108.
55. V. Pradeepa, S. Senthil-Nathan, S. Sathish-Narayanan, S. Selin-Rani, P. Vasantha-Srinivasan, A. Thanigaivel et al. (2016). Potential mode of action of a novel plumbagin as a mosquito repellent against the malarial vector *Anopheles stephensi* (Culicidae: Diptera). *Pest Biochem. Physiol.* **134**, 84–93.
56. S. P. Priya, S. Sakinah, K. Sharmilah, R. A. Hamat, Z. Sekawi, A. Higuchi, M. P. Ling, S. A. Nordin, G. Benelli and S. S. Kumar (2017). Leptospirosis: molecular trial path and immunopathogenesis correlated with malaria and dengue mimetic hemorrhagic infections. *Acta Trop.* **176**, 206–223.
57. R. Rajan, K. Chandran, S.L. Harper, S.I. Yun and P.T. Kalaichelvan (2015). Plant extract synthesized nanoparticles: an ongoing source of novel biocompatible materials. *Ind. Crops Prod.* **70**: 356–373.
58. A. Reegan, M. Rajiv Gandhi and M. G. Paulraj (2014). Ovicidal and oviposition deterrent activities of medicinal plant extracts against *Aedes aegypti* L. and *Culex quinquefasciatus* Say mosquitoes (Diptera: Culicidae). *Osong Public Health Res. Perspect.* **6**, 64–69.
59. A. Reegan, R. Vinoth Kannan, M. G. Paulraj and S. Ignacimuthu (2014). Synergistic effects of essential oil-based cream formulations against *Culex quinquefasciatus* Say and *Aedes aegypti* L. (Diptera: Culicidae). *J. Asia Pac. Entomol.* **17**, 327–331.
60. J. Rubio-Piña and F. Vázquez-Flota (2013). Pharmaceutical applications of the benzylisoquinoline alkaloids from *Argemone mexicana* L. *Curr. Top. Med. Chem.* **13**, 2200–2207.
61. R. B. Salunkhe, S. V. Patil, C. D. Patil and B. K. Salunke (2011). Larvicidal potential of silver nanoparticles synthesized using fungus *Cochliobolus lunatus* against *Aedes aegypti* (Linnaeus, 1762) and *Anopheles stephensi* Liston (Diptera; Culicidae). *Parasitol. Res.* **109**, 823–831.
62. G. Scrinis and K. Lyons (2007) The emerging nano-corporate paradigm: nanotechnology and the transformation of nature, food and agrifood systems. *Int. J. Sociol. Food Agric.* **15**, 1–23.
63. S. Senthil-Nathan (2013). Physiological and biochemical effect of neem and other Meliaceae plants secondary metabolites against Lepidopteron insects. *Front. Physiol.* **359**, 1–17.
64. S. Senthil-Nathan, A Review of Biopesticides and Their Mode of Action against Insect Pests, In: *Environmental Sustainability-Role of Green Technologies* (Springer, Berlin, 2015), pp. 49–63.
65. S. Sivapriyajothi, P. Mahesh Kumar, K. Kovendan and J. Subramaniam (2014). Larvicidal and pupicidal activity of synthesized silver nanoparticles using *Leucas aspera* leaf extract against mosquito vectors, *Aedes aegypti* and *Anopheles stephensi*. *J. Entomol. Acarol. Res.* **46**, 1787.
66. Stuart, B.H., 2002. *Polymer Analysis*. John Wiley & Sons, United Kingdom.
67. J. Subramaniam, K. Murugan, C. Panneerselvam, K. Kovendan, P. Madhiyazhagan, P. M. Kumar, D. Dinesh, B. Chandramohan, U. Suresh, M. Nicoletti, A. Higuchi, J. S. Hwang, S. Kumar, A. A. Alarfaj, M. A. Munusamy, R. H. Messing and G. Benelli (2016a). Eco-friendly control of malaria and arbovirus vectors using the mosquitofish *Gambusia affinis* and ultra-low dosages of *Mimusops elengi*-synthesized silver nanoparticles: towards an integrative approach? *Environ. Sci. Pollut. Res.* **22**, 20067–20083. doi:10.1007/s11356-015-5253-5
68. J. Subramaniam, K. Murugan, C. Panneerselvam, K. Kovendan, P. Madhiyazhagan, D. Dinesh, P. Mahesh, B. Chandramohan, U. Suresh, R. Rajaganesh, M. Saleh Alsalihi, S. Devanesan, M. Nicoletti, A. Canale and G. Benelli (2016b). Multipurpose effectiveness of *Couroupita guianensis*-synthesized gold nanoparticles: high antiplasmodial potential, field efficacy against malaria vectors and synergy with *Aplocheilus lineatus* predators. *Environ. Sci. Poll. Res.* **23**, 7543–7558. doi:10.1007/s11356-015-6007-0.
69. A. Suganya, K. Murugan, K. Kovendan, P. Mahesh and J. S. Hwang (2013). Green synthesis of silver nanoparticles using *Murraya koenigii* leaf extract against *Anopheles stephensi* and *Aedes aegypti*. *Parasitol. Res.* **112**, 1385–1397.
70. V. Sujitha, K. Murugan, M. Paulpandi, C. Panneerselvam, U. Suresh, M. Roni et al. (2015). Green-synthesized silver nanoparticles as a novel control tool against dengue virus (DEN-2) and its primary vector *Aedes aegypti*. *Parasitol. Res.* **114**, 3315–3325.
71. U. Suresh, K. Murugan, G. Benelli, M. Nicoletti, D. R. Barnard and C. Panneerselvam (2015). Tackling the growing threat of dengue: *Phyllanthus niruri*-mediated synthesis of silver nanoparticles and their mosquitocidal properties against the dengue vector *Aedes aegypti* (Diptera: Culicidae). *Parasitol. Res.* **114**, 1551–1562.
72. J. C. Tarafdar, S. Sharma and R. Raliya (2013). Nanotechnology: interdisciplinary science of applications. *Afr. J. Biotechnol.* **12**, 219–226.
73. A. Thanigaivel, P. Vasantha-Srinivasan, S. Senthil-Nathan, E. S. Edwin, A. Ponsankar, M. Chellappandian, S. Selin-Rani, J. Lija-Escaline and K. Kalaivani (2017). Impact of *Terminalia chebula* Retz. Against *Aedes aegypti* L. and non-target aquatic predatory insects. *Ecotoxicol. Environ. Saf.* **137**, 210–217.
74. S. Varun, S. Sellappa, M. Rafiqkhan and S. Vijayakumar (2015). Green synthesis of gold nanoparticles using *Argemone mexicana* L. leaf extract and its characterization. *Int. J. Pharm. Sci. Rev. Res.* **32**, 42–44.
75. R. Vidhyalakshmi, R. Bhagyaraj and R. S. Subhasree (2009). Encapsulation: the future of probiotics—a review. *Adv. Biol. Res.* **3**, 96–103.
76. K. Vikram, B. N. Nagpala, V. Pande, A. Srivastava, R. Saxena, and A. Anvikar (2016). An epidemiological study of dengue in Delhi, India. *Acta Trop.* **153**, 21–27.
77. V. Vogel, *Text book of practical organic chemistry* (The English Language Book Society and Longman, London, 1978), pp. 1368.
78. W. Ward and G. Benelli (2017). Avian and simian malaria: do they have a cancer connection? *Parasitol. Res.* **116**, 839–845.
79. T. C. Weeraratne, M. D. B. Perera and M. Mansoor (2013). Prevalence and breeding habitats of the dengue vectors *Aedes aegypti* and *Aedes albopictus* (Diptera: Culicidae) in the semi-urban areas of two different Climatic zones in Sri Lanka. *Int. J. Trop. Insect Sci.* **9**, 1–11.
80. J. Whitehorn and J. Farrar. (2010). Dengue. *Br. Med. Bull.* **95**, 161–173.
81. WHO, *Dengue and Severe Dengue. Factsheet no. 117* (World Health Organization, Geneva, 2015).